

# Interplay between Coulomb and Jahn-Teller effects in icosahedral systems with triplet electronic states coupled to $h$ -type vibrations

Haifa S. Alqannas, Andrew J. Lakin, Joseph A. Farrow, and Janette L. Dunn\*

*School of Physics and Astronomy, University of Nottingham, Nottingham NG7 2RD, United Kingdom*

(Received 12 June 2013; revised manuscript received 10 October 2013; published 31 October 2013)

We will consider the role played by electron-vibration and electron-electron interactions, through Jahn-Teller (JT) and Coulomb interactions, respectively, in icosahedral systems in which triplet electronic states are coupled to  $h_g$ -type vibrations. Starting from the electronic terms that arise from consideration of Coulomb interactions, we introduce JT couplings both within the terms and between nondegenerate terms. We show how the symmetry of the JT distortion can change when extra electrons are added, and give the conditions under which JT distortions can be suppressed entirely when the Coulomb interactions are sufficiently large. The relevance of our results to anions of the fullerene molecule  $C_{60}$  are briefly discussed, and existing experimental measurements are used to estimate values for the quadratic JT coupling constants for these anions.

DOI: [10.1103/PhysRevB.88.165430](https://doi.org/10.1103/PhysRevB.88.165430)

PACS number(s): 31.30.-i, 71.70.Ej, 61.48.-c

## I. INTRODUCTION

When an icosahedral molecule contains partially filled degenerate orbitals, coupling between the electrons and vibrations will want to cause a spontaneous distortion to a lower symmetry through the Jahn-Teller (JT) effect. However, where there is more than one electron present, electron-electron interactions also need to be considered. These will suppress potential JT distortions if they are sufficiently large or if they result in a singlet ground state, and can potentially alter the symmetry of the distortion in other cases. In this paper, we will consider the interplay between the JT and electron-electron interactions and the effect on the symmetry reduction for multiply occupied triplet electronic states coupled to fivefold vibrations. These are known as  $p^n \otimes h$  JT systems,<sup>1,2</sup> where electron-electron interactions must also be considered for  $n$  between 2 and 4. (For  $n = 5$ , the system is equivalent to having one hole and there is only one degenerate term, and for  $n = 6$ , the orbital is completely filled and there are no JT effects.)

The  $p^n \otimes h$  JT system is of interest from a fundamental theoretical point of view. Icosahedral symmetry is the highest possible point-group symmetry, and this results in features that do not occur in other systems. For example, the  $H \otimes h$  JT system was the first known example in which the dynamic JT effect can result in a change in the symmetry of the ground state (from a fivefold  $H$  state to a singlet).<sup>3,4</sup> The  $p^n \otimes h$  system is also of interest because it applies to anions of the fullerene molecule  $C_{60}$ , whose lowest-unoccupied molecular orbital (LUMO) is a  $T_{1u}$  state. The JT effect is believed to play an important role in the mechanisms behind why the  $A_3C_{60}$  fullerides can be superconducting up to relatively high temperatures,<sup>5-12</sup> whereas the  $A_4C_{60}$  fullerides are insulators. However, the role of the JT effect is not fully understood. It is therefore important to have a good fundamental understanding of the JT systems involved in general terms so that the role of the JT effect in determining properties of the fullerides can be understood.

Basic considerations of  $p^n \otimes h$  JT effects have been given in a number of papers. Some analytical and numerical work on solving these systems was first undertaken in Refs. 1 and 2, with further analytical and numerical considerations given in Refs. 11-19. Most recently, the possible symmetries of minima in the  $p^3 \otimes h$  system have been investigated.<sup>20</sup>

In all of the  $p^n \otimes h$  JT systems, linear coupling results in a continuous trough of minimum-energy points in the adiabatic potential energy surface (APES). Quadratic coupling, which is described by two independent coupling parameters (because the Kronecker product  $H \otimes H$  contains  $H$  twice),<sup>1,2</sup> warps this minimum-energy surface to produce a discrete set of minimum-energy points with the symmetry of one of the subgroups  $D_{5d}$ ,  $D_{3d}$ ,  $D_{2h}$ , or  $C_{2h}$  of the icosahedral group.<sup>1,2,19-21</sup> The system will move dynamically between the equivalent distortions, typically on a femtosecond time scale. The only exception to this is when there is a specific relationship between the two quadratic constants, when a trough of minimum-energy points remains.

Despite the above work, the influence of the Coulomb interaction on the symmetry of distortion has not previously been considered in significant detail. In this paper, we give a comprehensive investigation of the distortional symmetry for the different charge states, comparing results across the different systems. We show how, for given values of the quadratic coupling, inclusion of Coulomb interactions alters the symmetry compared to that which would be obtained due to the JT effect alone. We also give conditions under which the Coulomb interaction can suppress the symmetry reduction entirely.

As the strength of the quadratic coupling increases, the nuclear vibrations have a larger effect on the overall energy of the molecule. There are upper limits on the magnitude of the quadratic coupling parameters for which a JT system is intrinsically stable.<sup>20,22</sup> At the limit, the amplitudes of the vibrations become infinitely large and the system can be thought of as breaking apart, with the JT energy (i.e., the energy lowering compared to the value that would be obtained in the absence of JT effects) diverging to negative infinity. All couplings inside the limit result in a system stable with respect to nuclear displacements and with bounded JT energies. The limits will also be investigated as part of our symmetry analysis.

## II. THEORETICAL FORMALISM

### A. Hamiltonians for $p^n \otimes h$ systems

We wish to formulate the problem in which both inter-electron (Coulomb) interactions and electron-vibration (JT)

interactions are taken into account. According to the adiabatic approximation, the electronic part of the problem should first be solved for fixed nuclear positions and the effect of nuclear displacements added afterwards.<sup>23,24</sup> For the systems under consideration here, this means first determining the electronic terms that result from the interelectron interactions. JT effects are then incorporated using basis states representing the terms. This is the usual approach for combining interelectron and JT interactions,<sup>1,2</sup> which has been used in a number of previous works.<sup>1,2,15–20,24</sup> Starting from this basis, Hamiltonians can be constructed that incorporate the interelectron interactions by placing different terms at different energies. Additional contributions to the Hamiltonian are then added to incorporate JT interactions within the terms and between coupled terms. As different terms are nondegenerate, the JT interactions coupling different terms together can be viewed as being pseudo-JT (PJT) interactions.

For  $p^2 \otimes h$  and  $p^4 \otimes h$ , there is a high-spin term  ${}^3P$  transforming as  $T_1$ , and low-spin terms  ${}^1S$  and  ${}^1D$ , which transform as  $A$  and  $H$ , respectively. There is JT coupling within the  ${}^3P$  and  ${}^1D$  states (but not the  ${}^1S$  state as it is a singlet). In addition, the low-spin terms are coupled together by the PJT effect. However, they are not coupled to the high-spin term so the high- and low-spin contributions can be treated as two independent problems.

For  $p^3 \otimes h$ , Coulomb interactions result in a high-spin term  ${}^4S$ , which as it is an orbital singlet has no JT coupling, and low-spin terms  ${}^2P$  and  ${}^2D$  transforming as  $T_1$  and  $H$ , respectively.<sup>1,2</sup> The JT couplings within both the  $T_1$  and  $H$  states are found to be zero,<sup>1,2</sup> as noted previously in other contexts.<sup>25,26</sup> However, the PJT coupling between the  $T$  and  $H$  states is nonzero.

In the above bases, the total Hamiltonian in all cases can be written in the form

$$\mathcal{H}_{\text{tot}} = \mathcal{H}_{\text{int}} + \mathcal{H}_{\text{vib}} + \mathcal{H}_{\text{term}}. \quad (1)$$

Here,  $\mathcal{H}_{\text{term}}$  puts the different terms at different energies, as is usual in a PJT formalism. It is diagonal in our basis constructed from terms. For  $p^2 \otimes h$  and  $p^4 \otimes h$ , we will take the  ${}^1S$  state to be at an energy  $\delta_2$  relative to  ${}^1D$ , and for  $p^3 \otimes h$  we will take the  ${}^2P$  state to be at energy  $\delta_3$  relative to  ${}^2D$ .  $\mathcal{H}_{\text{vib}}$  represents the kinetic and potential energy terms describing the fivefold  $h$  vibration in terms of simple harmonic oscillators.  $\mathcal{H}_{\text{int}}$  incorporates all JT and PJT interactions, and can be written in the form

$$\mathcal{H}_{\text{int}} = V_1 \mathcal{H}_1 + V_2 \mathcal{H}_2 + V_3 \mathcal{H}_3, \quad (2)$$

where  $V_1$  is the linear JT coupling constant, and  $V_2$  and  $V_3$  are two independent quadratic coupling constants that arise due to the nonsimple irreducibility of the product  $H \otimes H$ .  $\mathcal{H}_1$  is a Hamiltonian incorporating JT and PJT interactions that are linear in the normal mode coordinates, and  $\mathcal{H}_2/\mathcal{H}_3$  incorporate interactions quadratic in these coordinates.

Following previous work,<sup>19,21</sup> we will label the normal mode coordinates as  $\{Q_\theta, Q_\epsilon, Q_4, Q_5, Q_6\}$ , where  $Q_4$ ,  $Q_5$ , and  $Q_6$  transform as the  $d$ -orbital functions  $d_{yz}$ ,  $d_{zx}$ , and  $d_{xy}$ , respectively. In cubic systems, it is usual to take  $\theta$  and  $\epsilon$  to transform as the  $d$ -orbital functions  $d_{3z^2-r^2}$  and  $d_{x^2-y^2}$ , respectively. The same choice can be made in these icosahedral systems, and indeed this may be a sensible choice when quadratic terms are neglected.<sup>15</sup> However, when quadratic

coupling is included, the expressions for minima in the APES in  $T \otimes h$  and  $p^2 \otimes h$  are found to be simpler if we use the Boyle and Parker convention,<sup>27</sup> which takes  $Q_\theta$  and  $Q_\epsilon$  to transform as

$$\begin{aligned} d_\theta &= \sqrt{\frac{3}{8}} d_{3z^2-r^2} + \sqrt{\frac{5}{8}} d_{x^2-y^2}, \\ d_\epsilon &= \sqrt{\frac{3}{8}} d_{x^2-y^2} - \sqrt{\frac{5}{8}} d_{3z^2-r^2}. \end{aligned} \quad (3)$$

This also allows direct use of the Clebsch-Gordon (CG) coefficients in Ref. 28 when setting up the interaction Hamiltonians.

Explicit forms for  $\mathcal{H}_1$ ,  $\mathcal{H}_2$ , and  $\mathcal{H}_3$  were constructed, using the definitions and CG coefficients described above, for  $p^1 \otimes h$  ( $T \otimes h$ ) in Ref. 21, for  $p^2 \otimes h$  in Ref. 19, and for  $p^3 \otimes h$  in Ref. 20. These papers all used basis functions for the  $D$  terms that transform in the same way as the  $Q$ s. The same Hamiltonians will be used for the starting point in this paper.

## B. Consistent definitions of JT coupling constants

As each of the previous papers on the  $p^n \otimes h$  systems mentioned above only looked at a specific number of electrons, no attempt was made to make the definitions of the coupling constants  $V_i$  consistent across the different systems. As the aim of the current paper is to see how the symmetry changes when we change the charge state, it is appropriate to work with consistent definitions. Although changing to consistent definitions is not an essential step in our work, it will allow us to predict how the symmetry of a given system will change when we change the number of electrons, as the values of the coupling constants themselves are not expected to change significantly when the number of electrons changes.

One way of obtaining consistent definitions of the coupling constants is to evaluate reduced matrix elements to link the different cases.<sup>1</sup> However, a simpler way is to write the basis states that describe the terms  ${}^2P$ ,  ${}^1D$ , etc., in the form of appropriate antisymmetrized combinations of products of single-electron  $T_{1u}$  states. We can then determine matrix elements using the results of operating on the single-electron states with a Hamiltonian which is like that for  $T \otimes h$  but where the interaction part is summed over  $n$  electrons.<sup>24</sup> The results can then be compared with the Hamiltonians found previously using the CG coefficients in Ref. 28. The Hamiltonians only differ by a constant factor. As a result, we find that we need to redefine  $V_1 \rightarrow -\sqrt{2/5}V_1$ ,  $V_2 \rightarrow -\sqrt{2/5}V_3$ , and  $V_3 \rightarrow -\sqrt{2/5}V_2$  in the low-spin  $p^2 \otimes h$  system compared to Ref. 19 to be consistent with the definitions used in the  $T \otimes h$  system.<sup>29</sup>  $V_2$  and  $V_3$  are interchanged because the columns of CG coefficients to which the couplings refer were interchanged in Ref. 19 compared to Ref. 29 for  $T \otimes h$ . The same replacements should be made for  $p^4 \otimes h$ , which contains two holes rather than two electrons. The high-spin  ${}^3P$  term is a triplet coupled to  $h$ -type vibrations; the result is equivalent to that of the single-electron  $T \otimes h$  problem except that the JT coupling constants are the negative of those for  $T \otimes h$ . For  $p^3 \otimes h$ , the definitions of the  $V_2$  and  $V_3$  used in Ref. 20 need to be interchanged to be consistent with those used for  $T \otimes h$ ,<sup>21</sup> although the numerical factors are consistent in this case. In all cases, the results for the coupling constants agree with those

TABLE I. Conditions to generate wells of a given symmetry from  $Q_\theta$ ,  $Q_\epsilon$ , and  $Q_6$  in all  $p^n \otimes h$  systems.

Symmetry	Condition
$D_{5d}$	$Q_\theta = 0, Q_\epsilon = \pm\sqrt{\frac{2}{3}}Q_6$
$D_{3d}$	$Q_\epsilon = 0, Q_\theta = \pm\sqrt{2}Q_6$
$D_{2h}$	$Q_6 = 0$
$C_{2h}$	None

found previously for linear coupling by evaluating reduced matrix elements, although the Hamiltonians themselves are different because of the different basis used.<sup>1,2</sup>

For the rest of this paper, we will use dimensionless coupling constants  $V'_i = V_i/(\mu\omega^2)$  ( $i = 1$  to 3), where the  $V_i$  relate to the new definitions above. We will also use dimensionless forms of the term splittings  $\delta'_i = \mu\omega^2\delta_i/V_1^2$ , where  $\mu$  is the mass and  $\omega$  the frequency of the  $h_g$  mode, which gives the strength of the Coulomb interactions relative to the strength of the linear JT coupling.

### C. Symmetry considerations

Group theoretical calculations dictate that for all of the  $p^n \otimes h$  systems, the symmetry is likely to reduce from  $I_h$  to  $D_{5d}$ ,  $D_{3d}$ ,  $D_{2h}$ , or  $C_{2h}$ . From group theory, it is possible for the symmetry to reduce further, e.g., to  $C_i$ , but detailed investigations have shown that the symmetry is never lower than  $C_{2h}$  in any of these systems (see Ref. 21 for  $n = 1$ , Ref. 19 for  $n = 2$  and 4, and Ref. 20 for  $n = 3$ ). Furthermore, applying operations of the icosahedral group to the  $Q_\gamma$  ( $\gamma \in \{\theta, \epsilon, 4, 5, 6\}$ ) shows that at least one minimum of each of  $D_{5d}$ ,  $D_{3d}$ ,  $D_{2h}$ , and  $C_{2h}$  can be found that involves just  $Q_\theta$ ,  $Q_\epsilon$ , and  $Q_6$ , so we can set  $Q_4 = Q_5 = 0$ .<sup>18</sup> Further conditions to generate minima of a given symmetry are given in Table I.<sup>18</sup> Using these conditions greatly simplifies the problem of finding JT minima, as instead of minimizing the energy with respect to the five  $Q_\gamma$ , it is only necessary to carry out a minimization in one dimension (for  $D_{5d}$  /  $D_{3d}$  symmetry), two dimensions (for  $D_{2h}$  symmetry), or three dimensions (for  $C_{2h}$ ).

Distortions to  $D_{5d}$ ,  $D_{3d}$ , and  $D_{2h}$  can be obtained by distorting along fivefold, threefold, or twofold axes (respectively) in the  $x$ - $y$  plane with respect to an icosahedron with a twofold  $z$  axis. These axes are shown in Fig. 1, with a circle in the  $x$ - $y$  plane also drawn as a guide to the eye. Distortions along any other axis through the center of the icosahedron and in the  $x$ - $y$  plane generate JT wells of  $C_{2h}$  symmetry. Equivalent planes (i.e., those including four corners of an icosahedron and through its center) also give minima of the above symmetries. Some consequences of this will be discussed in the following sections.

## III. SYMMETRY REGIONS

The ranges of JT parameters for which JT distortions can occur when there is one electron coupled to  $h$ -type vibrations (the  $T \otimes h$  case), and the symmetries that the distortions result in, have been studied previously.<sup>22</sup> We will now investigate the combined effects of JT and Coulomb interactions when

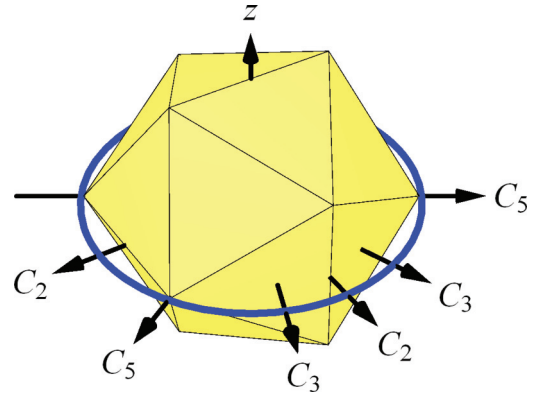


FIG. 1. (Color online) Locations of twofold, threefold, and fivefold distortional axes in the  $x$ - $y$  plane of an icosahedron (marked with a circle) with a twofold  $z$  axis. There are two axes each of each symmetry in this plane. Distortions along these axes correspond to JT minima of  $D_{2h}$ ,  $D_{3d}$ , and  $D_{5d}$  symmetry, respectively. Equivalent axes occur in other planes, giving a total of six fivefold axes, ten threefold axes, and 15 twofold axes. Distortions along all other axes in the  $x$ - $y$  plane (and equivalent planes) give wells of  $C_{2h}$  symmetry.

there is more than one electron, determining the effect on the symmetry reduction and the ranges of parameters for which JT distortions occur. As  $p^4 \otimes h$  is equivalent to  $p^2 \otimes h$ , it is only necessary to explicitly consider the  $p^2 \otimes h$  and  $p^3 \otimes h$  systems.

### A. $p^2 \otimes h$ system

As mentioned previously, the high-spin term  $^3P$  results in an identical JT system to that for  $T \otimes h$ ,<sup>21,22</sup> but with the signs of the coupling constants reversed. Therefore, the ranges of coupling constants over which JT effects can occur, and the symmetry of the minima obtained, will not be considered any further here. On the other hand, the additional complications introduced by considering Coulomb interactions in the two low-spin terms ( $^1D$  and  $^1S$ ) coupled by the JT effect has received much less attention. Investigations of the effect of the splitting between these two terms are the main aim of this section. However, it is first useful to consider the case of zero term splitting, as we will find that there are strong similarities between this case and that of  $T \otimes h$ , although we do not expect this situation to apply to real systems.

When  $Q_4 = Q_5 = 0$ , the electronic state corresponding to the minimum-energy just involves  $A$ ,  $H_\theta$ ,  $H_\epsilon$ , and  $H_6$ , thus reducing the dimension of the interaction matrix from  $6 \times 6$  to  $4 \times 4$ . We can write this matrix in terms of matrix elements  $H_{ij}$  for a modified  $T \otimes h$  problem with twice the interaction contribution (i.e.,  $V_i$  replaced by  $2V_i$ ), to allow for the addition of the extra electron. Here,  $i$  and  $j$  run from 1 to 3, corresponding to  $x$ ,  $y$ , and  $z$ . Without substituting the specific form for the  $H_{ij}$ , we find that three of the eigenvalues are identical to the three eigenvalues in the modified  $T \otimes h$  problem. The remaining eigenvalue is equivalent to  $(H_{11} + H_{22})$ .

For the  $T \otimes h$  problem, it was possible to find analytical expressions for the positions of minimum-energy wells in the APES and the corresponding JT energies and electronic states for almost all valid values of the quadratic coupling constants.

TABLE II. Coordinates  $Q_\gamma$  (in units of  $V_1'$ ) and the  $H$  components of the electronic states for  $D_{2h}$  minima in the  $p^2 \otimes h$  problem when the term splitting  $\delta_2'$  is zero. In all cases, the  $A$  component of the electronic state is  $-1/\sqrt{3}$ .  $\xi$  and  $\kappa$  are functions of  $V_2'$  and  $V_3'$ , as given in the text.  $\phi$  is the golden ratio  $\frac{1}{2}(1 + \sqrt{5})$ .

Label	Normal mode coordinates $\{Q_\theta, Q_\epsilon, Q_4, Q_5, Q_6\}$	Electronic state $\{H_\theta, H_\epsilon, H_4, H_5, H_6\}$
A	$\{\xi, \kappa, 0, 0, 0\}$	$\frac{1}{2}\{1, -\sqrt{\frac{5}{3}}, 0, 0, 0\}$
B	$\frac{1}{4}\{-\sqrt{3}\kappa - \xi, \kappa - \sqrt{3}\xi, -\sqrt{6}\kappa + \sqrt{2}\xi, 2\sqrt{2}\xi, -\sqrt{6}\kappa - \sqrt{2}\xi\}$	$\frac{1}{4}\{\phi^{-1}, -\frac{\phi^2}{\sqrt{3}}, \sqrt{2}\phi, 2\sqrt{2}, \sqrt{2}\phi^{-1}\}$
C	$\frac{1}{4}\{-\sqrt{3}\kappa - \xi, \kappa - \sqrt{3}\xi, \sqrt{6}\kappa - \sqrt{2}\xi, 2\sqrt{2}\xi, \sqrt{6}\kappa + \sqrt{2}\xi\}$	$\frac{1}{4}\{\phi^{-1}, -\frac{\phi^2}{\sqrt{3}}, -\sqrt{2}\phi, 2\sqrt{2}, -\sqrt{2}\phi^{-1}\}$
D	$\frac{1}{4}\{-\sqrt{3}\kappa - \xi, \kappa - \sqrt{3}\xi, \sqrt{6}\kappa - \sqrt{2}\xi, -2\sqrt{2}\xi, -\sqrt{6}\kappa - \sqrt{2}\xi\}$	$\frac{1}{4}\{\phi^{-1}, -\frac{\phi^2}{\sqrt{3}}, -\sqrt{2}\phi, -2\sqrt{2}, \sqrt{2}\phi^{-1}\}$
E	$\frac{1}{4}\{-\sqrt{3}\kappa - \xi, \kappa - \sqrt{3}\xi, -\sqrt{6}\kappa + \sqrt{2}\xi, -2\sqrt{2}\xi, \sqrt{6}\kappa + \sqrt{2}\xi\}$	$\frac{1}{4}\{\phi^{-1}, -\frac{\phi^2}{\sqrt{3}}, \sqrt{2}\phi, -2\sqrt{2}, -\sqrt{2}\phi^{-1}\}$
F	$\frac{1}{4}\{2\xi, -2\kappa, -\sqrt{6}\kappa - \sqrt{2}\xi, \sqrt{6}\kappa - \sqrt{2}\xi, -2\sqrt{2}\xi\}$	$\frac{1}{4}\{1, \sqrt{\frac{5}{3}}, \sqrt{2}\phi^{-1}, -\sqrt{2}\phi, -2\sqrt{2}\}$
G	$\frac{1}{4}\{2\xi, -2\kappa, -\sqrt{6}\kappa - \sqrt{2}\xi, -\sqrt{6}\kappa + \sqrt{2}\xi, 2\sqrt{2}\xi\}$	$\frac{1}{4}\{1, \sqrt{\frac{5}{3}}, \sqrt{2}\phi^{-1}, \sqrt{2}\phi, 2\sqrt{2}\}$
H	$\frac{1}{4}\{2\xi, -2\kappa, \sqrt{6}\kappa + \sqrt{2}\xi, -\sqrt{6}\kappa + \sqrt{2}\xi, -2\sqrt{2}\xi\}$	$\frac{1}{4}\{1, \sqrt{\frac{5}{3}}, -\sqrt{2}\phi^{-1}, \sqrt{2}\phi, -2\sqrt{2}\}$
I	$\frac{1}{4}\{2\xi, -2\kappa, \sqrt{6}\kappa + \sqrt{2}\xi, \sqrt{6}\kappa - \sqrt{2}\xi, 2\sqrt{2}\xi\}$	$\frac{1}{4}\{1, \sqrt{\frac{5}{3}}, -\sqrt{2}\phi^{-1}, -\sqrt{2}\phi, 2\sqrt{2}\}$
J	$\frac{1}{4}\{\sqrt{3}\kappa - \xi, \kappa + \sqrt{3}\xi, -2\sqrt{2}\xi, \sqrt{6}\kappa + \sqrt{2}\xi, -\sqrt{6}\kappa + \sqrt{2}\xi\}$	$\frac{1}{4}\{-\phi, \frac{\phi^{-2}}{\sqrt{3}}, -2\sqrt{2}, -\sqrt{2}\phi^{-1}, \sqrt{2}\phi\}$
K	$\frac{1}{4}\{\sqrt{3}\kappa - \xi, \kappa + \sqrt{3}\xi, 2\sqrt{2}\xi, \sqrt{6}\kappa + \sqrt{2}\xi, \sqrt{6}\kappa - \sqrt{2}\xi\}$	$\frac{1}{4}\{-\phi, \frac{\phi^{-2}}{\sqrt{3}}, 2\sqrt{2}, -\sqrt{2}\phi^{-1}, -\sqrt{2}\phi\}$
L	$\frac{1}{4}\{\sqrt{3}\kappa - \xi, \kappa + \sqrt{3}\xi, 2\sqrt{2}\xi, -\sqrt{6}\kappa - \sqrt{2}\xi, -\sqrt{6}\kappa + \sqrt{2}\xi\}$	$\frac{1}{4}\{-\phi, \frac{\phi^{-2}}{\sqrt{3}}, 2\sqrt{2}, \sqrt{2}\phi^{-1}, \sqrt{2}\phi\}$
M	$\frac{1}{4}\{\sqrt{3}\kappa - \xi, \kappa + \sqrt{3}\xi, -2\sqrt{2}\xi, -\sqrt{6}\kappa - \sqrt{2}\xi, \sqrt{6}\kappa - \sqrt{2}\xi\}$	$\frac{1}{4}\{-\phi, \frac{\phi^{-2}}{\sqrt{3}}, -2\sqrt{2}, \sqrt{2}\phi^{-1}, -\sqrt{2}\phi\}$
N	$\frac{1}{2}\{\sqrt{3}\kappa - \xi, -\kappa - \sqrt{3}\xi, 0, 0, 0\}$	$\frac{1}{2}\{-\phi, -\frac{\phi^{-2}}{\sqrt{3}}, 0, 0, 0\}$
O	$\frac{1}{2}\{-\sqrt{3}\kappa - \xi, -\kappa + \sqrt{3}\xi, 0, 0, 0\}$	$\frac{1}{2}\{\phi^{-1}, \frac{\phi^2}{\sqrt{3}}, 0, 0, 0\}$

This gave minima of  $D_{5d}$ ,  $D_{3d}$ , or  $D_{2h}$  symmetry, depending on the values of the quadratic coupling. The only exception to this was a very small range of couplings for which  $C_{2h}$  minima were obtained. In this region, the results could only be obtained numerically.<sup>21,22</sup> Substituting explicit forms for  $H_{11}$  and  $H_{22}$  allows us to obtain an analytical solution for the minimum energy of the additional solution that occurs in the low-spin  $p^2 \otimes h$  system. We find that this corresponds to a  $D_{2h}$  point which can never be a global minimum. Therefore, the minimum-energy eigenvalues of  $p^2 \otimes h$  are identical to those of the modified  $T \otimes h$  system. This can be seen to be true symbolically from the results in Ref. 19, after applying the appropriate transformations of the  $V_i$ . We have also confirmed this result numerically by minimizing the lowest eigenvalue of the complete  $p^2 \otimes h$  Hamiltonian with respect to the  $Q_\gamma$  for specific values of  $V_2'$  and  $V_3'$ .

Analytical expressions for the energy, vibrational coordinates, and electronic states of minima of  $D_{2h}$  symmetry, which have not been presented previously, are given in Table II. In this table,

$$\xi = -\sqrt{\frac{3}{2}} \frac{(1 + \sqrt{2}V_2' + \sqrt{2/5}V_3')}{1 - 4V_2'^2/5 - 12V_3'^2/5}, \quad (4)$$

$$\kappa = \sqrt{\frac{5}{2}} \frac{(1 + 3\sqrt{2/5}V_3' - \sqrt{2}V_2'/5)}{1 - 4V_2'^2/5 - 12V_3'^2/5}.$$

The 15  $D_{2h}$  wells have been labeled A to O in a manner that is consistent with Ref. 30 for the  $(h_u^+)^2 \otimes h_g$  system, although the values of  $\xi$  and  $\kappa$  are different in the two systems.

It is not possible to obtain analytical expressions for the minima when the term splitting is included because the equations are too complicated and it is not possible to make a

comparison with the  $T \otimes h$  case, where there is no equivalent to the term splitting. However, the  $Q_\gamma$  must take the same symbolic form as without the term splitting as this is a general requirement in order to obtain points of the stated symmetry. For example, the  $Q_\gamma$  for the  $D_{2h}$  minima take the same symbolic form as in Table II but where  $\xi$  and  $\kappa$  are no longer given by the expressions in Eq. (4).

The ranges of  $V_2'$  and  $V_3'$  which give stable JT distortions, and the symmetries of the minima in those cases, have not previously been investigated for  $p^2 \otimes h$ . From the analogy to  $T \otimes h$ , it follows that when the term splitting is zero, the shape of the region of validity, and the dependence of the symmetries of the minima on the quadratic coupling, must be the same as given in the Appendix of Ref. 22 but with the  $V_i'$  scaled by a factor of 2 due to the different definitions of the coupling constants. We then consider the case of nonzero term splitting. We know that for any point on the boundary of the region of validity for the JT Hamiltonian only, the lowest eigenvalue, which is the JT energy  $E_{JT}$ , must tend to  $-\infty$ . From general properties of Hermitian matrices,<sup>31</sup> it follows that the energy with the term splitting included must be less than or equal to  $E_{JT} + \lambda$ , where  $\lambda$  is the lowest eigenvalue of the term splitting Hamiltonian (namely 0 if  $\delta_2'$  is positive or  $\delta_2'$  if  $\delta_2'$  is negative). Therefore, this must also tend to  $-\infty$  for all points on the boundary of the JT-only problem. Thus the same boundary must hold both with and without the term splitting. In fact, the same must be true for any extra interaction introduced to the system, as long as its largest eigenvalue is bounded above as  $(V_2', V_3')$  tends to a point on the boundary. This result has also been checked numerically.

Once the region in which  $V_2'$  and  $V_3'$  are valid has been established, the dependence on  $V_2'$  and  $V_3'$  of the type of symmetry reduction can be found for any given value of

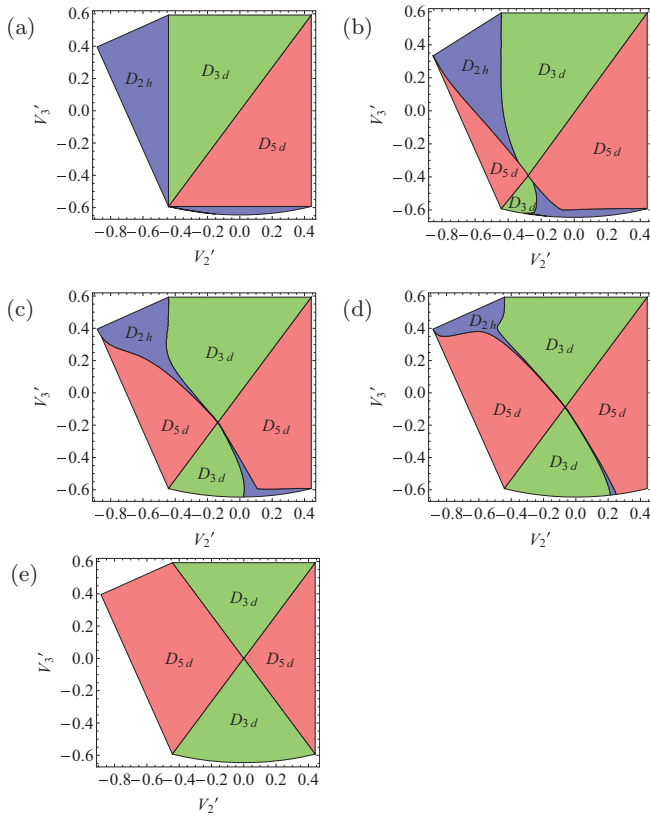


FIG. 2. (Color online) Symmetry region plot for the low-spin  $p^2 \otimes h$  problem with different term splittings that place the  $A$  state above or equal to the  $H$  state ( $\delta'_2 \geq 0$ ): (a)  $\delta'_2 = 0$ , (b)  $\delta'_2 = 0.24$ , (c)  $\delta'_2 = 0.96$ , (d)  $\delta'_2 = 2.4$ , (e)  $\delta'_2$  infinite. The unmarked region below the rightmost  $D_{5d}$  region in (a) to (d) (blue online) is of  $D_{2h}$  symmetry.

the term splitting  $\delta'_2$ . This was done by performing a three-dimensional minimization (in  $Q_\theta$ ,  $Q_\epsilon$ , and  $Q_6$ ) over a coarse grid of points. The boundaries between regions found to be of  $D_{5d}$ ,  $D_{3d}$ , and  $D_{2h}$  symmetry were then determined more accurately by performing much quicker one-dimensional minimizations to obtain the energies of minima of  $D_{5d}$  and  $D_{3d}$  symmetry, and a two-dimensional minimization for  $D_{2h}$ . It is necessary to perform longer three-dimensional minimizations in the vicinity of borders with the  $C_{2h}$  region to determine the extent of this region more accurately.

The symmetry regions are displayed in Figs. 2(a) to 2(e) for  $\delta'_2 = 0, 0.24, 0.96, 2.4$ , and  $\infty$ , respectively. The result for  $\delta'_2 = 0$  is the same as in Ref. 22, but is repeated here for comparison purposes. It should be noted that there is a small  $C_{2h}$  region between the lower  $D_{2h}$  region and the limit of validity, with  $-0.88 < V'_2 < -0.30$ . This region, which can only be discerned as a slight thickening of the boundary line in Fig. 2(a), can be seen in more detail in Ref. 22. For  $\delta'_2 = 0.24$ , there is also a very small  $C_{2h}$  region bounded by the border of validity and the lower  $D_{2h}$  region, between approximately  $V'_2 = -0.61$  and  $-0.34$ . This has a maximum width of less than 0.01, and can again only be discerned as a slightly thickened line on the scale of the plots. A more detailed view of this region is not presented here as the region is negligibly small and on the border of validity, such that it is extremely unlikely that any real system would have coupling constants

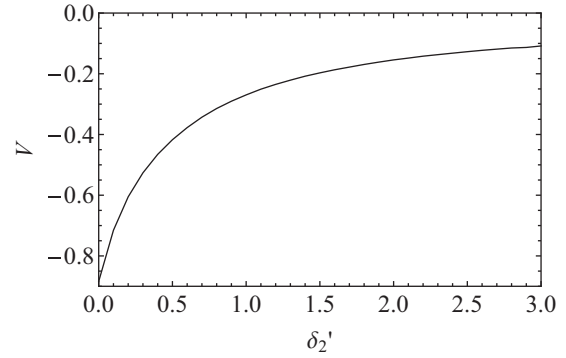


FIG. 3. Dependence on the term splitting  $\delta'_2$  and the quadratic coupling constant  $V = 2V'_2 = (2\sqrt{5}/3)V'_3$  of the point where multiple regions of different symmetries meet in the low-spin  $p^2 \otimes h$  system.

that would place it in this region. The results for  $\delta_2 \rightarrow \infty$  in Fig. 2(e) is obtained by taking the Hamiltonian to be the  $5 \times 5$  block that is obtained when the  $A$  state is omitted.

Clear trends can be seen in the plots as  $\delta'_2$  increases from zero. Increasing  $\delta'_2$  introduces additional  $D_{5d}$  and  $D_{3d}$  regions that are not present at  $\delta'_2 = 0$ , with a corresponding decrease in the sizes of the  $D_{2h}$  regions. The  $D_{2h}$  regions vanish completely in the limit of infinite  $\delta'_2$ . The line  $V'_3 = \frac{3}{\sqrt{5}}V'_2$ , which divides regions of different symmetries in all cases, corresponds to a continuous trough of minimum-energy points of accidentally higher symmetry than any of the point groups we consider. There is a point on this line where multiple regions of different symmetry meet. At  $\delta'_2 = 0$ , this point starts at the lower left-hand corner of the line, and moves up the line as  $\delta'_2$  increases, asymptotically approaching  $V'_2 = V'_3 = 0$  in the limit of  $\delta'_2 \rightarrow \infty$ , as shown in Fig. 3.

We now consider the case of negative  $\delta'_2$ . For small negative values of  $\delta'_2$ , the region plot looks very similar to that for the corresponding positive value of  $\delta'_2$ . For example, the plot for  $\delta'_2 = -0.24$  is almost indistinguishable from that in Fig. 2(b), with just a very small shift in the lower boundary between  $D_{3d}$  and  $D_{2h}$ . Here, although the  $A$  state is lowest in energy, it is sufficiently close to the  $H$  state for a JT effect in the combined  $A-H$  system to operate. JT effects continue to operate for all values of  $V'_2$  and  $V'_3$  with  $\delta'_2 > -0.4$ . However, for more negative values of  $\delta'_2$ , a JT effect can only operate for larger values of quadratic coupling. For smaller values of quadratic coupling, the  $A$  state is sufficiently low in energy to suppress all JT effects.

The boundaries between both the  $D_{5d}$  and  $D_{3d}$  regions and the region in which no JT effect operates can both be seen to be solutions of the equation

$$5(175 + 400\delta'_2 + X) + 8V[\sqrt{2}(X - 10 - 100\delta'_2) - 16V(1 + 10\delta'_2)] = 0, \quad (5)$$

where

$$X = \sqrt{25(73 + 160\delta'_2) - 16V(5\sqrt{2} + 8V)(20\delta'_2 - 1)}, \quad (6)$$

and where setting the quadratic coupling  $V = 2V'_2$ ,  $(2\sqrt{5}/3)V'_3$ , or  $-5/(4\sqrt{2}) - 2V'_2$  generates the rightmost  $D_{5d}$ , the  $D_{3d}$ , and the leftmost  $D_{5d}$  borders, respectively. The boundaries with  $D_{2h}$  regions can be found numerically,

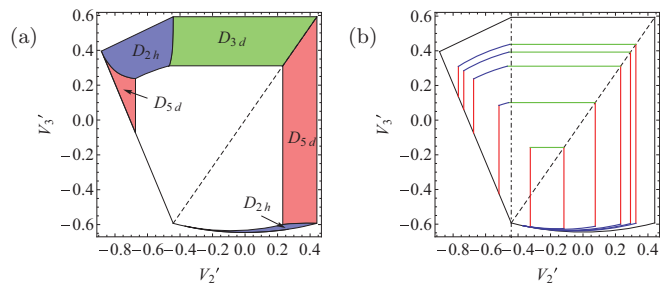


FIG. 4. (Color online) (a) Symmetry region plot for the  $p^2 \otimes h$  problem with a term splitting  $\delta'_2 = -0.75$ . In the white region, the  $A$  state is lowest in energy and no JT effect operates. (b) Regions in which no JT effect operates for different negative values of the term splitting  $\delta'_2$ . The excluded regions are those inside the truncated rectangular regions with  $\delta'_2 = -0.41, -0.5, -0.75, -1.0$ , and  $-1.25$  from the smallest region to the largest region, respectively. In each case, the upper horizontal line (green online) is the boundary with the  $D_{3d}$  region, the vertical lines (red online) are the boundaries with  $D_{5d}$ , and the curved lines (blue online) are boundaries with  $D_{2h}$ . The dashed line is the line  $V'_3 = (3/\sqrt{5})V'_2$ , and the dot-dashed line is  $V'_2 = -5/(8\sqrt{2})$ .

although the equations involved are rather more complicated. The overall region in which no JT effect operates, and the symmetry of the minima in regions where a JT effect is still present, is shown in Fig. 4(a) for  $\delta'_2 = -0.75$ . The dependence on  $\delta'_2$  of the size of the central region where there is no JT effect is shown in Fig. 4(b), with values of  $\delta'_2$  from  $-0.41$  to  $-1.25$ . It is found that the  $D_{5d}$  boundaries are placed symmetrically around the value  $V'_2 = -5/(16\sqrt{2})$ , marked as a dot-dashed line in Fig. 4(b). This is the value of  $V'_2$  at which the borders first appear when  $\delta'_2 = -0.4$ , and is the average value of  $V$  for the two  $D_{5d}$  borders in Eq. (5).

The increase in size of the excluded region slows as  $\delta'_2$  becomes more negative, with much larger increases in the magnitude of  $\delta'_2$  required for a given increase in the excluded area than for smaller values. The limit of no JT effect for any values of quadratic coupling is only approached asymptotically as  $\delta'_2 \rightarrow -\infty$ . Furthermore, the boundaries all approach their outer limits at the same rate. The variation of the value of quadratic coupling at which JT effects cease to operate is shown in Fig. 5. This is different from the behavior at small negative values of  $\delta'_2$ , where there is a precise value of  $\delta'_2$  (namely  $-0.4$ ) at which JT effects first start to disappear, rather than an asymptotic limit. This corresponds to  $V'_2 \approx -0.221$ . The significance of the change in symmetry or suppression of symmetry reduction when an additional electron is added will be discussed later in relation to the fullerene molecule  $C_{60}$ .

### B. $p^3 \otimes h$ system

Here, we need to consider PJT coupling between  $T_{1u}$  and  $H_u$  states.<sup>1,26</sup> This means that to search for minima in the lowest APES, we need to find eigenvalues of the  $8 \times 8$  matrix formed from the combined  $T_{1u}$  and  $H_u$  basis. However, as before, we can set  $Q_4 = Q_5 = 0$  to find at least one minimum of each of the  $D_{5d}$ ,  $D_{3d}$ ,  $D_{2h}$ , and  $C_{2h}$  symmetries. In this case, the matrix is found to be simpler if we define

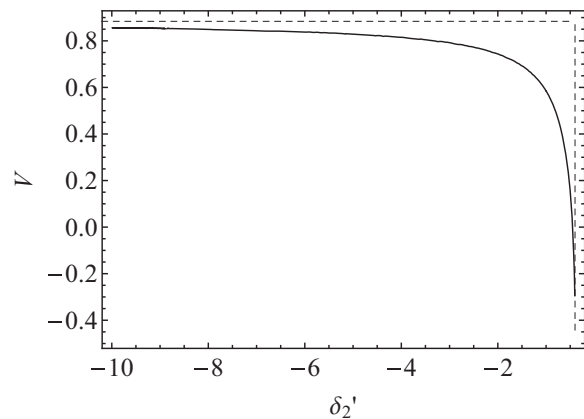


FIG. 5. Dependence of the value of quadratic coupling at which the JT effect ceases to operate as a function of  $\delta'_2$  for  $p^2 \otimes h$ . Here,  $V = 2V'_2$ ,  $(2\sqrt{5}/3)V'_3$ , or  $-5/(4\sqrt{2}) - 2V'_2$ . The upper dashed line is the limit of  $5/(4\sqrt{2})$  that forms the outer boundary of the region of validity, which is approached asymptotically. The rightmost dashed line is the value  $\delta'_2 = -0.4$  at which an excluded region first appears.

the  $\theta$  and  $\epsilon$  components of the  $H_u$  basis to transform as  $d_{3z^2-r^2}$  and  $d_{x^2-y^2}$ , respectively. This reduces the problem to independent  $4 \times 4$  and  $3 \times 3$  matrices and a diagonal element  $(Q_\theta^2 + Q_\epsilon^2 + Q_6^2)/2$ . Analytical expressions can be found for the eigenvalues as functions of the  $Q_\gamma$ , which was not possible in  $p^2 \otimes h$  despite the lower dimension of the matrix. The result is two possible minimum-energy eigenvalues of the form

$$E_i = l - \frac{1}{2}\sqrt{m_i + \delta_3^2}, \quad (7)$$

where  $l = \frac{1}{2}(Q_\theta^2 + Q_\epsilon^2 + Q_6^2 + \delta_3^2)$ ,  $m_1 = \frac{24}{5}Q^2$ , and  $m_2 = \frac{6}{5}(Q' + \sqrt{3}|Q'_{\theta d}|)^2$ , with  $Q' = \sqrt{Q_\theta^2 + Q_\epsilon^2}$ , where  $Q'_{\theta d} = \sqrt{\frac{3}{8}}Q'_\theta - \sqrt{\frac{3}{8}}Q'_\epsilon$  and  $Q'_{\epsilon d} = \sqrt{\frac{5}{8}}Q'_\theta + \sqrt{\frac{3}{8}}Q'_\epsilon$  are combinations that relate to the  $d$ -orbital definitions of  $\theta$  and  $\epsilon$ , and where

$$\begin{aligned} Q'_6 &= Q_6 \left( 1 - \sqrt{2}V'_2 Q_\epsilon + \sqrt{\frac{2}{3}}V'_3 Q_\theta \right), \\ Q'_\theta &= Q_\theta + \frac{V'_2}{\sqrt{2}}Q_\theta Q_\epsilon + \frac{V'_3}{2\sqrt{6}}(3(Q_\theta^2 - Q_\epsilon^2) + 2Q_6^2), \\ Q'_\epsilon &= Q_\epsilon + \frac{V'_2}{2\sqrt{2}}((Q_\theta^2 - Q_\epsilon^2) - 2Q_6^2) - \sqrt{\frac{3}{2}}V'_3 Q_\theta Q_\epsilon \end{aligned} \quad (8)$$

(in units of  $V'_1$ ). Note that although the forms for  $E_1$  and  $E_2$  are simplest when written using the  $d$ -orbital definitions of  $\theta$  and  $\epsilon$ ,  $Q'_{\theta d}$  and  $Q'_{\epsilon d}$  themselves are simplest when written in terms of  $Q_\theta$  and  $Q_\epsilon$  [as in Eq. (8)] rather than their  $d$ -orbital equivalents. For the solution  $E_2$ , the magnitude of the ratio of the contributions of states  $T_{1ux}$  and  $T_{1uy}$  to the eigenstate is the same as that for the ratio of  $H_4$  and  $H_5$ , which is not altogether surprising as the pairs of states have similar transformation properties. More explicitly, the eigenstate can be written as

$$\psi = \{\cos \beta \cos \alpha, \pm \cos \beta \sin \alpha, \mp \sin \beta \cos \alpha, \sin \beta \sin \alpha\} \quad (9)$$

with respect to the basis  $\{T_{1ux}, T_{1uy}, H_4, H_5\}$ , where  $\alpha$  is a parameter relating to the ratio of the contributions from the pairs of state of a given transformation property and  $\beta$  relates the mixing between the  $T$  and  $H$  states. When  $\delta'_3 = 0$ , both states contribute equally and so  $\beta = \pi/4$ .

Linear coupling results in a trough in the lowest APES, with quadratic coupling introducing minima, as for the other  $p^n \otimes h$  systems.<sup>1,17</sup> However, the minima are of  $C_{2h}$  symmetry for most values of quadratic coupling, with some small regions of quadratic coupling giving  $D_{2h}$  symmetry. This is different to the predominantly  $D_{5d}$  and  $D_{3d}$  symmetries seen in the other systems.<sup>20</sup>

It is not possible to write down analytical expressions for the minimum energies, but solutions can be easily found by numerically minimizing  $E_1$  and  $E_2$  with respect to the  $Q_\gamma$ . First, it is useful to note that the minima for couplings  $(V'_2, V'_3)$  are the same as those for  $(-V'_2, -V'_3)$ . This is because it can be shown mathematically that  $E_1$  and  $E_2$  are invariant under the simultaneous transformations  $\{V'_2 \rightarrow -V'_2, V'_3 \rightarrow -V'_3, Q_\theta \rightarrow -Q_\theta, Q_\epsilon \rightarrow -Q_\epsilon\}$ . Therefore the minimum energies for points  $(V'_2, V'_3)$  and  $(-V'_2, -V'_3)$  will be the same (just corresponding to vibrational coordinates  $Q_\theta$  and  $Q_\epsilon$  of the opposite signs). The energy expressions are also invariant under the transformation  $\delta'_3 \rightarrow -\delta'_3$ , apart from a constant term involving  $\delta'_3$  only. Hence identical types of minima will be obtained for equivalent positive and negative values of  $\delta'_3$ . Both of these features reduce the number of situations that need to be considered numerically.

Another difference between  $p^3 \otimes h$  and the  $p^2 \otimes h$  and  $p^4 \otimes h$  systems is that there are no JT effects for large ranges of JT coupling parameters when the term splitting is either a large positive or a large negative number. This is because there are no ‘‘diagonal’’ JT couplings within either the  $T_{1u}$  or the  $H_u$  states, so that when either the  $T_{1u}$  or the  $H_u$  state is significantly lower in energy than the other state, the coupling between the states becomes very small. While this has been noted before,<sup>20</sup> no attempt has been made to determine the size or shape of the JT-excluded region for different values of  $\delta'_3$ , so this is what we will look at now.

Figure 6 shows the values of coupling constants for which JT effects are possible at different values of  $\delta'_3$ . The outer boundary shows the limits beyond which no JT effects are possible, whatever the value of  $\delta'_3$ . Some inner regions are also excluded when  $|\delta'_3| \approx 2.4$  and above. The solid inner curves show the bounds of JT-excluded regions for  $\delta'_3 = \pm 2.5$  (innermost curves),  $\delta'_3 = \pm 3$  (middle curves), and  $\delta'_3 = \pm 4$  (outer curves). Inside these regions, the term splitting dominates over the JT effect such that no JT distortions are possible. Also shown in the figure are the areas of  $D_{2h}$  symmetry for  $\delta'_3 = 0$  (the shaded areas touching the diagonal line) and for  $\delta'_3 = \pm 3$  (the remaining shaded areas). The most notable feature here is that, where JT minima exist, the term splitting has very little effect on the symmetry of the minima. This is different from  $p^2 \otimes h$  and  $p^4 \otimes h$ , where the symmetry at given coupling constants showed a much greater dependence on the term splitting. This is because the symmetry in  $p^3 \otimes h$  is predominantly  $C_{2h}$ , which can be achieved with distortions along a much greater range of axes than for distortions to the higher subgroups (as discussed in Sec. II C). Therefore the precise nature of the distortion can change with  $\delta'_3$  without

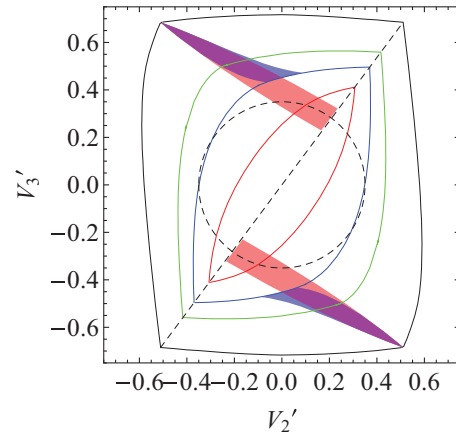


FIG. 6. (Color online) Symmetry region plot for  $p^3 \otimes h$ . The region inside the innermost solid lines (red online) has no JT effects for  $\delta'_3 = \pm 2.5$ . The region inside the next-outermost solid lines (blue online) is excluded for  $\delta'_3 = \pm 3$ , and the region inside the next solid lines (green online) is excluded for  $\delta'_3 = \pm 4$ . The outermost solid lines (black online) shows the outer border of validity for any JT effects. The shaded areas abutting the diagonal line (pink online) show the  $D_{2h}$  region for  $\delta'_3 = 0$ , with the remaining shaded areas (blue online) showing the  $D_{2h}$  regions for  $\delta'_3 = \pm 3$ . The remaining areas are of  $C_{2h}$  symmetry. The dashed line is the line  $V'_3 = (3/\sqrt{5})V'_2$ , and the dashed circle is  $V_{\text{tot}} = 0.35$ .

the resulting symmetry changing. Classification of the type of  $C_{2h}$  distortion when  $\delta'_3 = 0$  in terms of the axes of distortion was discussed in Ref. 20.

Equation (7) showed that mathematically there are two possible forms for the energy eigenvalue that can be lowest in energy. It can be seen that for the  $D_{2h}$  regions (where  $Q'_6 = 0$ ), both expressions give the same minimum energy. Numerical investigations show that  $E_2$  gives a lower energy for the majority of the remaining ranges of quadratic coupling. There are four small regions of quadratic coupling where the minimum energy comes from  $E_1$ , which all correspond to large values of quadratic coupling near to the outer limit of validity. Figure 7 shows the results for  $\delta'_3 = 0$ . Results for other values of  $\delta'_3$  are identical to this to within calculational error, which is not surprising as  $\delta'_3$  appears in  $E_1$  and  $E_2$  in the same way. It is therefore most likely that the expression  $E_2$  will be most relevant for any real system. However, the minimum energies from the two solutions are relatively close, so that the presence of additional interactions could alter the ordering.

To further investigate the symmetry of possible JT distortions and the effect of the term splitting, it is useful to consider the variation in the JT energy assuming  $D_{2h}$  and  $C_{2h}$  distortions for a fixed magnitude of quadratic coupling by setting  $V'_2 = V_{\text{tot}} \cos \beta$  and  $V'_3 = V_{\text{tot}} \sin \beta$ .  $\beta$  is a mixing angle that determines the contributions of the  $V'_2$  and  $V'_3$  couplings to the total quadratic coupling. The results for four different values of  $\delta'_3$  when  $V_{\text{tot}} = 0.35$  are shown in Fig. 8. It is only necessary to consider  $\beta$  between  $-\pi/2$  and  $+\pi/2$  (which is equivalent to  $V'_2 \geq 0$ ), rather than a full range of  $2\pi$ , as remaining values can be obtained by symmetry from these values.

The plots in Figs. 8(a) to 8(c) show that there are ranges of  $\beta$  where  $D_{2h}$  solutions are lowest in energy, and other ranges of

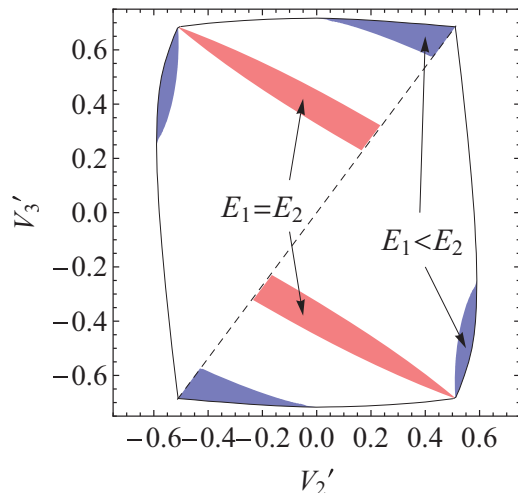


FIG. 7. (Color online) Comparison of the energies  $E_1$  and  $E_2$  when  $\delta'_3 = 0$ . The shaded regions near the outer boundary (blue online) are where  $E_1 < E_2$ . For the  $D_{2h}$  regions (red online), both energies are equal. For all other regions,  $E_1 > E_2$ .

$\beta$  for which  $C_{2h}$  solutions are lowest. For negative values of  $\beta$ , the  $D_{2h}$  and  $C_{2h}$  curves merge smoothly into each other. The  $Q_\gamma$  also smoothly merge, indicating that the JT distortional axes smoothly move from the  $C_2$  axes such as in Fig. 1. The point at positive  $\beta$  in (a) and (b) where the  $D_{2h}$  and  $C_{2h}$  curves meet corresponds to a point on the line  $V'_3 = (3/\sqrt{5})V'_2$ . The values of the  $Q_\gamma$  show distinct jumps for  $\beta$  either side of this point, indicating a corresponding jump in the orientation of the axis of distortion. Plots (c) and (d) show that there are ranges of  $\beta$  for which no JT solution exists for these values of  $\delta'_3$ . In plot (d), where the magnitude of the term splitting is relatively large, there are no  $D_{2h}$  solutions, and  $C_{2h}$  solutions only exist over a small range of  $\beta$ .

From Fig. 8, it can be seen that the results for  $\delta'_3 = \pm 2$  are very similar to those for  $\delta'_3 = 0$ , with just a slight rise

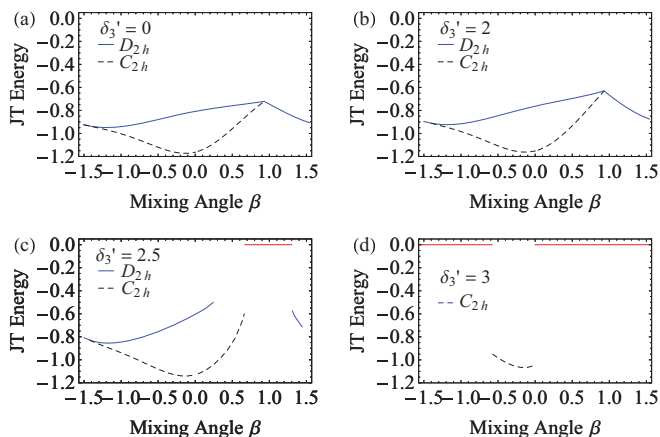


FIG. 8. (Color online) Variation of the JT energy as a function of the mixing angle  $\beta$  for the  $p^3 \otimes h$  problem, assuming either  $D_{2h}$  or  $C_{2h}$  distortions. All plots are for  $V_{\text{tot}} = 0.35$ . The four plots are for (a)  $\delta'_3 = 0$ , (b)  $\delta'_3 = \pm 2$ , (c)  $\delta'_3 = \pm 2.5$ , and (d)  $\delta'_3 = \pm 3$ . The horizontal lines at zero energy in (c) and (d) show ranges of  $\beta$  in which there are no JT effects.

in the energy values. In fact, results for all values of  $\delta'_3$  between these limits are very similar, showing that the term splitting has negligible effect on the results in this range. The situation is different for  $\delta'_3 = \pm 2.5$ , where JT effects have become excluded for some values of quadratic coupling. The results here can be related to Fig. 6, where the dashed circle shows  $V_{\text{tot}} = 0.35$ . It can be seen that the circle crosses the inner boundary of validity for  $\delta'_3 = \pm 2.5$  at  $\{V'_2, V'_3\} \approx \{\pm 0.10, \pm 0.34\}$  and  $\{\pm 0.28, \pm 0.21\}$ , which corresponds to  $\beta \approx 1.3$  and  $0.67$  (in the range  $-\pi/2 < \beta < \pi/2$ ), which is consistent with Fig. 8(c). For  $\delta'_3 = \pm 3$ , the dashed circle in Fig. 6 shows that JT effects are excluded for almost all quadratic couplings. This is also consistent with Fig. 8(d). For magnitudes of  $\delta'_3$  larger than this, all JT effects disappear for this value of  $V_{\text{tot}}$ .

#### IV. DISCUSSION

The results of the last section, taken all together, let us make some general conclusions about the JT effects that are to be expected in icosahedral systems with one or more electrons in an electronic  $T$  state and coupled to  $h$ -type vibrations. The JT coupling constants can be expected to have roughly the same values in all charge states, as they are fundamentally related to derivatives of the nuclear potential which are not related to the number of electrons. This lets us predict how the symmetry will change when the number of electrons changes. For example, a system with one electron would have JT distortions of  $D_{3d}$  symmetry if  $V'_2 = V'_3 = -0.6$ , as shown in Fig. 2(a). However, Figs. 2(c) to 2(e) show that if an extra electron is added to the same system, it would exhibit  $D_{5d}$  distortions if the low-spin states are sufficiently low in energy compared to the high-spin states and the term splitting between the (low-spin)  $A$  and  $H$  states is a sufficiently large positive value. On the other hand, if the high-spin states are sufficiently low in energy, the system would show  $D_{3d}$  distortions, as the mathematics of the JT problem would be the same as for a single electron. If the low-spin states are lowest in energy but the Coulomb interactions place the  $A$  state below the  $H$  states, there would be no JT interaction at all if the  $A-H$  energy gap is sufficiently large, as shown by Fig. 4.

For a system with three electrons, the JT effect is absent for a much wider range of coupling constants than for the other charge states, because the ranges of parameters over which a JT effect can occur are much less, as shown in Fig. 6. For example, if a third electron is added to a system with the same JT parameters as in the example above, there will be no JT distortion whatever the values of the Coulomb interactions between the  $A$ ,  $T$ , and  $H$  states. This is because there can never be a JT distortion if the  $A$  state is lowest in energy, and if it is higher in energy such that the low-spin  $T$  and  $H$  states are relevant, there will be no JT distortion either as  $V'_2 = V'_3 = -0.6$  lies beyond the outer bounds of validity.

The results we have presented can also be used to determine information on the values of the quadratic coupling constants for given systems based on known experimental observations. As an example, we will consider the fullerene anions  $C_{60}^{n-}$ . For the monoanion ( $n = 1$ ), interpretation of both the electronic spectra in solution<sup>32</sup> and gas phase spectra in a storage ring<sup>33</sup> require a  $D_{3d}$  distortion. Also, scanning



tunneling microscopy images of  $C_{60}$  molecules on an alkylthiol self-assembled monolayer<sup>34</sup> have been interpreted in terms of JT parameters that would cause a  $D_{3d}$  distortion (with an additional perturbation to further lower the symmetry due to interactions with the surface substrate).<sup>35</sup> Early semiempirical molecular orbital calculations also predicted  $D_{3d}$  symmetry,<sup>36</sup> as did density functional theory (DFT) calculations.<sup>37</sup> All of these results suggest that the quadratic coupling parameters in this problem must lie within the range of the green triangle in Fig. 2(a). Furthermore, *ab initio* Hartree-Fock calculations suggest that the energies of  $D_{5d}$ ,  $D_{3d}$ , and  $D_{2h}$  structures are very similar,<sup>38</sup> as do recent DFT calculations.<sup>39</sup> In our model, all three symmetries are found to have the same energy along the line  $V'_3 = (3/\sqrt{5})V'_2$ . This is actually a continuous trough of equivalent-energy points, including points of  $C_{2h}$  symmetry, although this might not be detected in numerical methods that only search for distortions of specific symmetries. Taken together, the experimental evidence and the results of these calculations suggest that the quadratic coupling parameters must be close to but slightly above the  $V'_3 = (3/\sqrt{5})V'_2$  line.

Recent calculations using DFT suggest that  $D_{2h}$  distortions are the most energetically favorable in the  $C_{60}^-$  ion, although as with the Hartree-Fock calculations, the energies of all three symmetry distortions were found to be fairly similar.<sup>40</sup> In our model, the only way the distortions could be of  $D_{2h}$  symmetry but with both the  $D_{5d}$  and  $D_{3d}$  distortions also having similar energies would be if the quadratic couplings are close to the lower-left corner in Fig. 2(a) [with  $V'_2 = -5/(8\sqrt{2}) \approx -0.44$  and  $V'_3 = -3\sqrt{5}/(8\sqrt{2}) \approx -0.59$ ] which, although possible, seems unlikely given all the other evidence for a  $D_{3d}$  distortion.

High-temperature spectroscopic data on  $K_4C_{60}$  and  $Rb_4C_{60}$  suggest that these materials contain  $C_{60}^{4-}$  ions that are decoupled from the lattice and act as isolated ions subject to dynamic JT distortions of  $D_{5d}$  or  $D_{3d}$  symmetry.<sup>41</sup> These results can both be explained by taking the same ranges of quadratic coupling constants that we have deduced hold for the monoanion if the Coulomb interactions result in a high-spin ground state, where the JT effect results in a  $T \otimes h$  problem with distortional symmetries as in Fig. 2(a). They also hold for a low-spin ground state, where the results of Figs. 2(b) to 2(e) or Fig. 4 hold, as long as the  $A$  state is either above the  $H$  state or at least not so far below the  $H$  state that JT effects are suppressed. We note that calculations indicate that, when JT effects are neglected, the high-spin state is lower than the low-spin states and the  $A$  state is above the  $H$  state.<sup>42</sup> Estimates in Ref. 32 of the JT energy in  $T \otimes h$  of around 58 meV lead to estimates of  $V_1^2/(\mu\omega^2) \approx 0.29$  eV, which from the values of the term splitting in Ref. 42 leads to an estimate of  $\delta'_3 \approx 0.98$ , meaning that the results in Fig. 2(c) will apply. The JT effect itself could alter the ordering of the high- and low-spin states,<sup>1,2</sup> but in either case the results are consistent with our requirements.

An alternative explanation of the results for  $C_{60}^{4-}$  would be for the low-spin states to dominate and the quadratic coupling constants to lie close to the regions where all three symmetries have similar energies, such as the top-left to bottom-right regions in Figs. 2(b) to 2(d). However, this would not be consistent with the results for  $C_{60}^-$  unless the results are also close to the line  $V'_3 = (3/\sqrt{5})V'_2$ . Note that the overall

symmetry of  $C_{60}^{4-}$  ions in a  $K_4C_{60}$  monolayer were assumed to be of  $D_{2h}$  symmetry from an analysis of STM images,<sup>39</sup> but the ions in the STM images are perturbed by interactions with the surface substrate and neighboring ions, so the experimental data cannot be used to deduce anything about the symmetry of isolated  $C_{60}^{4-}$  ions.

There is also evidence for a strong JT effect in  $C_{60}^{3-}$  ions in  $Cs_3C_{60}$ ,<sup>10</sup> but as these are not isolated from their neighbors it is not possible to make any further predictions about the quadratic coupling constants from this data. Calculations of the energies of the high- and low-spin states suggest that, in the absence of JT couplings, the high-spin singlet state would be lowest in energy,<sup>42</sup> which cannot be subject to a JT distortion. Using the same estimates of the linear JT coupling as above leads to an estimate of  $\delta'_3 \approx 0.66$  in this case. It is therefore possible that the JT effect could result in a change in the energy-level ordering so that a JT distortion can occur, but again no quantitative conclusions can be made.

## V. CONCLUSIONS

We have considered the interplay between JT effects and Coulomb interactions in triplet orbital levels coupled to fivefold vibrations. In the cases of two or four electrons, we find that JT distortions are suppressed when the  $^1S$  term is sufficiently lower in energy than the  $^1D$  term, but that distortions will always occur when the  $^1D$  term is lowest in energy. In contrast, when there are three electrons, PJT distortions will not occur if the Coulomb interaction is sufficiently strong that the splitting it induces is sufficiently large to prohibit significant mixing between the nondegenerate levels. This is true irrespective of whether the  $^2P$  or the  $^2D$  term is lowest in energy, and occurs because there is no JT coupling within either the  $^2P$  or  $^2D$  term. This suppression of a distortion when PJT coupling is insufficiently strong to overcome the barrier due to the separation of coupled nondegenerate levels is an expected feature of the PJT effect.<sup>24</sup> In this case, the effect of the PJT coupling is to alter the curvature of the lowest APES,<sup>24</sup> as indeed can also occur with regular JT effects.<sup>43</sup> However, this is a relatively subtle effect so has not been considered in this paper. Instead, we have concentrated on determining the conditions under which a distortion will occur.

Another difference between the different charge states is on the symmetry of possible JT distortions. For the three-electron case, the Coulomb interactions have very little effect on the symmetry, whereas for the two- and four-electron cases the symmetry depends on the strength of the Coulomb interaction for a wide range of quadratic JT coupling parameters. This means that adding charge to a system is more likely to alter the symmetry of distortion.

The results in this paper are expected to have relevance for ions of the fullerene molecule  $C_{60}$ , as well as other icosahedral molecules. As there is plenty of evidence that these ions are distorted, the results presented here are expected to apply. While the anion  $C_{60}^-$  is generally believed to be distorted to  $D_{3d}$  symmetry,<sup>32,33,37</sup> we have used estimates of the JT coupling constants from experimental evidence to show that this does not necessarily mean that higher charge states will also be distorted to  $D_{3d}$  symmetry.

## ACKNOWLEDGMENTS

A.J.L. and J.A.F. gratefully acknowledge the support of EPSRC (UK) for funding this work through a Doctoral

Training Account and vacation bursary, respectively. H.S.A. is grateful for funding from King Abdulaziz University in the Kingdom of Saudi Arabia.

\*janette.dunn@nottingham.ac.uk; <http://www.nottingham.ac.uk/~ppzjld>

<sup>1</sup>C. C. Chancey and M. C. M. O'Brien, *The Jahn-Teller Effect in C<sub>60</sub> and other Icosahedral Complexes* (Princeton University Press, Princeton, 1997).

<sup>2</sup>M. C. M. O'Brien, *Phys. Rev. B* **53**, 3775 (1996).

<sup>3</sup>C. P. Moate, M. C. M. O'Brien, J. L. Dunn, C. A. Bates, Y. M. Liu, and V. Z. Polinger, *Phys. Rev. Lett.* **77**, 4362 (1996).

<sup>4</sup>P. De Los Rios, N. Manini, and E. Tosatti, *Phys. Rev. B* **54**, 7157 (1996).

<sup>5</sup>C. M. Varma, J. Zaanen, and K. Raghavachari, *Science* **254**, 989 (1991).

<sup>6</sup>O. Gunnarsson, *Rev. Mod. Phys.* **69**, 575 (1997).

<sup>7</sup>A. L. Sobolewski, *Chem. Phys. Lett.* **267**, 452 (1997).

<sup>8</sup>J. E. Han, O. Gunnarsson, and V. H. Crespi, *Phys. Rev. Lett.* **90**, 167006 (2003).

<sup>9</sup>M. Capone, M. Fabrizio, C. Castellani, and E. Tosatti, *Rev. Mod. Phys.* **81**, 943 (2009).

<sup>10</sup>G. Klupp, P. Matus, K. Kamarás, A. Y. Ganin, A. McLennan, M. J. Rosseinsky, Y. Takabayashi, M. T. McDonald, and K. Prassides, *Nat. Commun.* **3**, 912 (2012).

<sup>11</sup>A. Auerbach, *Phys. Rev. Lett.* **72**, 2931 (1994).

<sup>12</sup>N. Manini, E. Tosatti, and A. Auerbach, *Phys. Rev. B* **49**, 13008 (1994).

<sup>13</sup>A. Auerbach, N. Manini, and E. Tosatti, *Phys. Rev. B* **49**, 12998 (1994).

<sup>14</sup>W. H. Green, S. M. Gorun, G. Fitzgerald, P. W. Fowler, A. Ceulemans, and B. C. Titeca, *J. Phys. Chem.* **100**, 14892 (1996).

<sup>15</sup>S. Sookhun, J. L. Dunn, and C. A. Bates, *Phys. Rev. B* **68**, 235403 (2003).

<sup>16</sup>J. L. Dunn and H. Li, *Phys. Rev. B* **71**, 115411 (2005).

<sup>17</sup>J. L. Dunn, *J. Phys.: Condens. Matter* **17**, 5499 (2005).

<sup>18</sup>I. D. Hands, J. L. Dunn, W. A. Diery, and C. A. Bates, *Phys. Rev. B* **73**, 115435 (2006).

<sup>19</sup>L. M. Sindi, I. D. Hands, J. L. Dunn, and C. A. Bates, *J. Mol. Struct.* **838**, 78 (2007).

<sup>20</sup>A. Lakin, I. D. Hands, C. A. Bates, and J. L. Dunn, in *Vibronic Interactions and the Jahn-Teller Effect: Theory and Applications*, Progress in Theoretical Chemistry and Physics, Vol. 23, edited by M. Atanasov and C. Daul (Springer, Dordrecht, 2012), pp. 231–243.

<sup>21</sup>J. L. Dunn and C. A. Bates, *Phys. Rev. B* **52**, 5996 (1995).

<sup>22</sup>I. D. Hands, J. L. Dunn, and C. A. Bates, *Phys. Rev. B* **82**, 155425 (2010).

<sup>23</sup>I. B. Bersuker and V. Z. Polinger, *Vibronic Interactions in Molecules and Crystals* (Springer-Verlag, Heidelberg, 1989).

<sup>24</sup>I. B. Bersuker, *The Jahn-Teller Effect* (Cambridge University Press, Cambridge, UK, 2006).

<sup>25</sup>F. G. Anderson, F. S. Ham, and G. Grossman, *Materials. Sci. Forum* **83-87**, 475 (1992).

<sup>26</sup>A. Ceulemans, *Top. Curr. Chem.* **171**, 27 (1994).

<sup>27</sup>L. Boyle and Y. M. Parker, *Mol. Phys.* **39**, 95 (1980).

<sup>28</sup>P. W. Fowler and A. Ceulemans, *Mol. Phys.* **54**, 767 (1985).

<sup>29</sup>J. L. Dunn, I. D. Hands, and C. A. Bates, *J. Mol. Struct.* **838**, 60 (2007).

<sup>30</sup>I. D. Hands, W. A. Diery, C. A. Bates, and J. L. Dunn, *Phys. Rev. B* **76**, 085426 (2007).

<sup>31</sup>W. Fulton, *Bull. Amer. Math. Soc.* **37**, 209 (2000).

<sup>32</sup>I. D. Hands, J. L. Dunn, C. A. Bates, M. J. Hope, S. R. Meech, and D. L. Andrews, *Phys. Rev. B* **77**, 115445 (2008).

<sup>33</sup>S. Tomita, J. U. Andersen, E. Bonderup, P. Hvelplund, B. Liu, S. B. Nielsen, U. V. Pedersen, J. Rangama, K. Hansen, and O. Echt, *Phys. Rev. Lett.* **94**, 053002 (2005).

<sup>34</sup>L.-F. Yuan, J. Yang, H. Wang, C. Zeng, Q. Li, B. Wang, J. G. Hou, Q. Zhu, and D. M. Chen, *J. Am. Chem. Soc.* **125**, 169 (2003).

<sup>35</sup>J. L. Dunn, A. J. Lakin, and I. D. Hands, *New J. Phys.* **14**, 083038 (2012).

<sup>36</sup>K. Tanaka, M. Okada, K. Okahara, and T. Yamabe, *Chem. Phys. Lett.* **193**, 101 (1992).

<sup>37</sup>M. Saito, *Phys. Rev. B* **65**, 220508 (2002).

<sup>38</sup>N. Koga and K. Morokuma, *Chem. Phys. Lett.* **196**, 191 (1992).

<sup>39</sup>A. Wachowiak, R. Yamachika, K. H. Khoo, Y. Wang, M. Grobis, D. H. Lee, S. G. Louie, and M. F. Crommie, *Science* **310**, 468 (2005).

<sup>40</sup>H. Ramanantoanina, M. Gruden-Pavlovic, M. Zlatar, and C. Daul, *Int. J. Quantum Chem.* **113**, 802 (2013).

<sup>41</sup>G. Klupp, K. Kamarás, N. M. Nemes, C. M. Brown, and J. Leão, *Phys. Rev. B* **73**, 085415 (2006).

<sup>42</sup>A. V. Nikolaev and B. N. Plakhotin, *Russ. Chem. Rev.* **79**, 729 (2010).

<sup>43</sup>Y. M. Liu, J. L. Dunn, C. A. Bates, and V. Z. Polinger, *J. Phys.: Condens. Matter* **9**, 7119 (1997).